PEROVSKITE SOLAR CELLS: A BRIEF INTRODUCTION AND SOME REMARKS

CELDAS SOLARES DE PEROVSKITAS: UNA BREVE INTRODUCCIÓN Y ALGUNAS CONSIDERACIONES

Osbel Almora[a†], L. Vaillant-Roca[b] and Germà Garcia-Belmonte[a]

a) Institute of Advanced Materials (INAM), Universitat Jaume I, 12006 Castelló, Spain; oalmora89@gmail.com†
b) Photovoltaic Research group, ENERMAT Division, Institute of Materials Science and Technology (IMRE) and Faculty of Physics, University of Havana, Cuba
† corresponding author

Recibido 8/5/2017; Aceptado 5/6/2017

The spectacular and unprecedented rise of so-called perovskite solar cells (PSCs) in conversion efficiency with low-cost manufacturing processes has grabbed the attention of the scientific community in the field of photovoltaics during the last four years. The inclusion of perovskite type absorber materials, typically $CH_3NH_3PbI_3$, has been the key factor for the development of this emerging technology that has created great of expectations. However, many poorly understood aspects of its operating modes still need convincing explanations. This paper provides a brief introduction to the structure, materials and characteristics of PSCs. In addition, some remarks about the stability of these devices are provided and the state-of-the-art of several subjects of interest is discussed, such as the hysteresis phenomenon of current-voltage curves.

El espectacular y sin precedentes ascenso de las llamadas celdas solares de perovskitas (PSCs, por sus siglas en inglés) en cuanto a eficiencia de conversión con procesos de fabricación de bajo presupuesto ha acaparado la atención de la comunidad científica en el campo de la fotovoltaica en los últimos cuatro años. La inclusión de materiales absorbedores tipo perovskita, típicamente el $CH_3NH_3PbI_3$, ha sido el factor clave para el desarrollo de esta tecnología emergente con la que se tienen muchas perspectivas. Sin embargo, no son pocos los aspectos de su funcionamiento que aún faltan por comprender. En este trabajo se brinda una breve introducción a la estructura, materiales y características de las PSCs. Además se comenta especialmente acerca de la estabilidad de estos dispositivos y se discuten varios temas de interés como el fenómeno de la histéresis de las curvas corriente-voltaje.

PACS: Efficiency and performance of solar cells, 88.40.hj; Organic-inorganic hybrid nanostructures, 81.07.Pr; Semiconductors thin films, 73.61.Jc; Reviews, 01.30.Rr.

I. INTRODUCTION

Photovoltaic (PV) technologies has received an incremental attention during the last decades as one of the most feasible options for humankind future sustainable development. In fact, it has been recently suggested [1] that PVs will account for 35 % of the additional electricity generation capacity installed globally by 2040. Nowadays, the current largest contributor to Si module price now comes from cell encapsulation [1]. Nevertheless, despite the manufacturing optimization, the fabrication process is still complex and expensive. Furthermore, it was only recently when a power conversion efficiency (PCE) of 26 % was achieved for Si cells [2] from a theoretical limit around 29 % [3].

Aiming at the reduction of costs and enhance versatility, newer technologies have been developed such as typical CdTe and CIGS thin film solar cells [4] or the so called emerging technologies, for instance, dye-sensitized solar cells (DSSCs) [5] and organic solar cells [6]. Nevertheless, possibly the most recent and promising PV devices are the denominated perovskite solar cells (PSCs), that in about four years have already achieved PCE larger than 22 % for laboratory cells [2] with a theoretical limit evaluated at 31 % [7]. These results match the current record for CdTe thin films solar cells, the second technology in the market and the one with lower manufacturing costs, which make the PV community believe in a prompt overpassing by PSCs. This is also endorsed by several potential applications such as: building integration in windows with transparency and/or colors, flexibility and high efficiency in tandem configuration assembly silicon technology.

The perovskites is the denomination of a wide family of materials with the general formula ABX_3 and the crystal structure of the mineral perovskite, the calcium titanate ($CaTiO_3$). Figure 1 illustrate such structure where the A cation is coordinated with twelve X ions and the B cation with six. Thus, the A cation is normally found to be somewhat larger than the B cation [8]. Several properties have been found for these materials for many years, e.g. ferroelectric, piezoelectric, ferromagnetic, antiferromagnetic, thermoelectric, insulating, semiconducting, conducting, superconducting and catalyst [9]. However, it was not until 2006 when PV application was first reported by Miyasaka and co-workers for devices with methylammonium lead halide perovskites $CH_3NH_3Pb(I_3, Br_3)$ as absorber material, proving less than 1 % of PCE for all solid-state cells [10]. These first works and further optimizations by Park and co-workers [11] resulted in the "perovskite phenomena" trigger when in 2012 up to 10 % efficiency $CH_3NH_3PbI_3$ [12] and mixed halide $CH_3NH_3PbI_{3-x}Cl_x$ [13] based solid-state devices were

obtained.

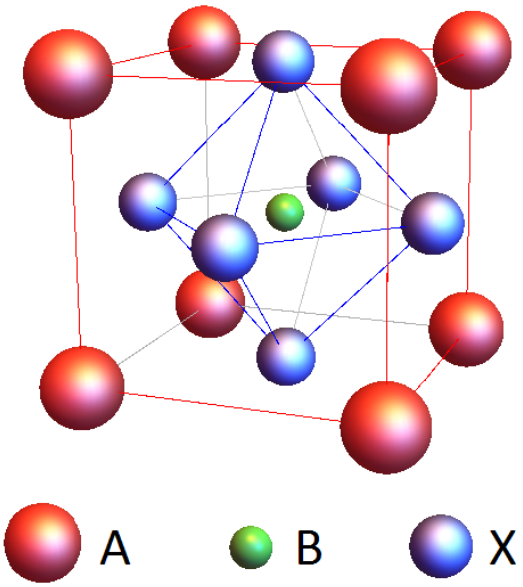

Figure 1. Generic perovskite ABX_3 crystal unit cell structure. In most typical PSCs A is the organic cation CH_3NH_3, B is the metallic cation Pb and X is the halide anion (I, Cl, Br or mixed).

In the present work a first approach survey on the structure, materials and characteristics of PSCs is provided. Consequently, especial attention is paid here to the issue of performance stabilization, which currently centers the most of attention among researchers in the field. Moreover, regarding the mechanisms behind the device operation, a discussion on the anomalous phenomenon of hysteresis in the current density-voltage ($J-V$) curve is presented, as well as its relation with other behaviors such as the low frequency capacitance [14] and the slow electrical material response under light irradiation [15]. Note that the manuscript is also intended to guide the readers throughout a selection of recent high impact original papers and review articles, as well as provide them with handy experimental data.

II. STRUCTURE OF PSCs

The PSCs structure basically consists in a light harvesting perovskite sandwiched between electrons and holes selective contacts. Several materials has been reported [16], however probably the most successful and extensively studied arrangement is that showed in Figure 2 where on top of the fluorine-doped tin oxide (FTO)/glass substrate the TiO_2 layer is grown, then the $CH_3NH_3PbI_3$ perovskite and later the spiro-OMeTAD. The metallic electrodes are often made of gold in order to achieve better connections with the load (R_{Load}), despite other non-precious metals has been also explored [17]. Thus, in this *regular* structure the light crosses the substrate throughout the glass and the transparent conducting oxide (TCO), then first through the electron-transport material (ETM) to be absorbed at the perovskite, the hole-transport material (HTM) being afterward in the light path.

In some devices, variations in the *regular* structure have been considered as the ETM (or HTM) free PSCs and the HTM free PSCs. Particularly pointed by Meng et al. [18], another important configuration is the *inverted*, where in the same light path direction the sequence of layers is *glass/TCO/HTM/perovskite/ETM/counter-electrode* [19]. In the review by Zhou et al. [20] the characteristics of all of these architectures are systematically analyzed.

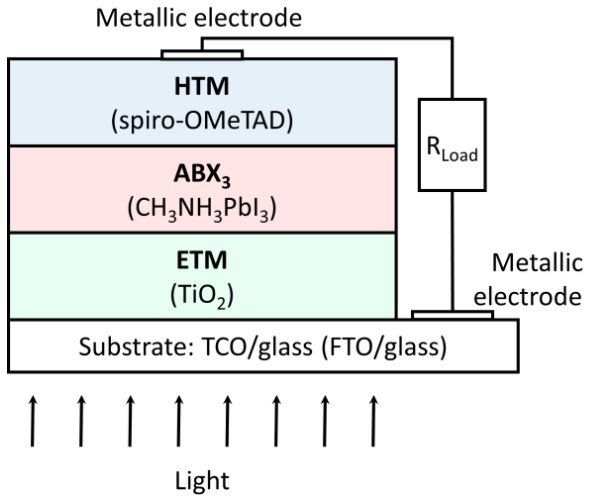

Figure 2. PSCs most typical (regular) structure.

II.1. The electron transport material

As indicated in Figure 2, the role of ETM is usually played by the TiO_2. This material is transparent to visible light, has low absorption and high refractive index (e.g. at $\lambda = 550$ nm the refractive index and the extinction coefficient are respectively $n = 2.54$ and $k < 10^{-4}$) [21] and it mainly occurs in three crystalline polymorphs: rutile (tetragonal), anatase (tetragonal), and brookite (orthorhombic). The rutile bulk phase is thermodynamically the most stable while anatase is the most interesting for use in high surface area photocatalytic and PV devices [22]. The anatase TiO_2 is an indirect bandgap semiconductor that presents intrinsic n-type conductivity [23]. The nature of this conductivity comes from oxygen vacancies and/or titanium interstitials and can be improved by the incorporation of shallow donor impurities (e.g., Nb, F, and H) [24]. For the donor carrier density of the order of 10^{18} cm^{-3} has been reported [25, 26] and, interestingly, it has being pointed that the distribution of these donors levels in the TiO_2 follows an exponential density of states (DOS) bellow the conduction band [27, 28].

Importantly, the layers of TiO_2 for PV applications can be grown by many low cost techniques (e.g. spin coating and spray pyrolysis [23]) obtaining crystalline films as well as nanostructured coatings (e.g. nanotubes, nanosheets, nanorods and nanofibers [29,30]) on top of the FTO. The work by He et al. [31] comments on several TiO_2 nanostructures for PSCs, despite that in regular structure it is presented in two main configurations: (i) as a flat compact layer and (ii) as

a mesoporous scaffold deposited on top of a planar compact film.

Among the different alternatives as ETM some examples can be mentioned: Al_2O_3 [32–34], SnO_2 [35–37], ZnO [38–41], ZrO_2 [42,43] and carbon/graphene derivatives [44–46]. About the latter, the works by Acik & Darling [44] and Covallini & Delgado [46] are illustrative.

Nonetheless, particular attention is paid here to the fullerene derivative PCBM, extensively used in organic solar cells (OSCs) [47] and typically employed as n-type electrode for the devices with inverted configuration. In its two flavours, the *[6,6]-phenyl-C-61-butyric acid methyl ester* ($PC_{60}BM$) and the *[6,6]-phenyl-C-71-butyric acid methyl ester* ($PC_{70}BM$), the PCBM film is deposited on top of the perovskite layer constituting the interface with the counter electrode. For this materials it is known that the relatively low electron mobility and relatively big size molecules influences the charge transporting and phase separation. Anyway, the optimization of the electron's selective extraction is currently a priority via the development of new materials and/or by modifying and/or mixing the already known ones. In connection to it, we list the review by Yang et al. [48].

II.2. The hole transport material

The characteristic HTM that is deposited above the perovskite in the regular configured PSCs is the *2,2'(7,7')-tetrakis-(N,N-di-p-methoxyphenyl - amine)9,9' - spiro-bifluorene*, earlier referred as spiro-OMeTAD (see Figure 2). This organic semiconductor has been extensively studied due to its applications as HTM in solid-state DSSCs [49]. In its pristine state, spiro-OMeTAD presents low intrinsic hole–mobility and –conductivity that has been found to increment the cell series resistance. Consequently the material needs to be p-doped to increase the charge carrier density. This occurs naturally during exposure to oxygen and light (so-called photodoping), nevertheless, several chemical dopants have been investigated to controllably oxidize the material [50,51].

Alternatively, among those used as hole-selective contacts, most of the reported materials are organics or hybrid compounds, as summarized by Calió et al. [52]. As inorganic HTMs we list here CuSCN [53,54], CuO_x [55], NiO_x [41,56] MoO_x [57] and VO_x [58], being CuO_x the one with best reported PCE, as highlighted in the survey by Rajeswari et al. [59].

At this point we once more emphasize on the predominant HTM in the PSCs with inverted structure: the *poly(3,4-ethylenedioxythiophene)* (PEDOT) doped with *poly(4-styrenesulfonate)* (PSS). The PEDOT:PSS is an oxidized electro-chemically stable conjugated polymer that has been extensively investigated given its applications in OSCs and light-emitting devices (p-LEDs) [60]. Its characteristic moderate transparency [60–62], that increases with polarization [63], allows to deposit it on top of the surface of indium tin oxide (ITO) letting the light pass for being absorbed at the perovskite, that is the next layer to be deposited in the inverted configuration.

II.3. The light harvesting material

Among perovskites it seems that the presence of halides is required when seeking PV applications, as pointed by Li et al. [64], and until now it is $CH_3NH_3PbI_3$ (referred as $MAPbI_3$ in the next) the most representative in this field. As systematically described by Stoumpos et al. [65], in its high temperature α cubic phase, the methyl ammonium organic cation CH_3NH_{3+} (MA) is A in the perovskite general formula while the lead and the halogen are B and X, respectively (see Figure 1).

The $MAPbI_3$ has been found to be a direct band-gap semiconductor [19, 66, 67] with high absorption coefficient ($10^4 - 10^5$ cm^{-1} in the visible range) [68, 69] and large carrier mobility ($\mu = 10^2 - 10^3$ $cm^2V^{-1}s^{-1}$) [65, 69]. The deposition of the material follows easy solution-based fabrication processes, e.g. dip and spin coating [68,70], and the layers can be obtained with good crystalline quality and at relatively high reaction rates, even when processed at low temperatures.

Importantly, the electrical intrinsic conductivity of $MAPbI_3$ can be modified from p-type to n-type by controlling growth conditions, i.e. by managing the concentration of donor or acceptor shallow defects [71]. Calculated transition energy levels of $MAPbI_3$ point defects in the literature [72, 74] have shown as dominant shallow levels close the valence band edge: the vacancies of lead (V_{Pb}) and methyl ammonium (V_{MA}) and the antisite substitution of MA in a lead site (MA_{Pb}). On the other hand, the shallow levels near the conduction band bottom are the iodine vacancies (V_I) and interstitial methyl ammoniums (MA_i). Other deep energy levels in the bandgap stand as Shockley-Read-Hall non-radiative recombination centers, which reduce minority carrier lifetimes, and therefore the open circuit voltage (V_{OC}) [75]; e.g. the donors interstitial leads (Pb_i) and leads in iodine sites (Pb_I), and the acceptors iodines in methyl ammonium ($_{MA}$) and lead (I_{Pb}) sites.

The tunable conductivity character of $MAPbI_3$ has produced a significant scattering in the representation of the energy band diagram of PSCs. In this context many studies have determined the work function of the different constituent layers via photoelectron spectroscopy and/or the measurement of the contact potential difference at the interfaces by using Kelvin probe force microscopy [27]. As result, and only citing a few examples, several works [71, 76–78] report that a p-n-n+ junction is formed by the p-HTM and the both n-type ETM and $MAPbI_3$, considering the depletion region towards the perovskite/HTM interface. Some other authors [26,71,79,80] have found a p-p-n junction considering a p-type $MAPbI_3$ with the consequent space charge region towards the perovskite/ETM interface. And a third group of publications [6,81,82] supports that a p-i-n junction, with intrinsic $MAPbI_3$, takes place in some PSCs. Anyway, it is clear that the fabrication procedure and the

interface engineering directly affects the conductivity, e.g. in the study by Wang et al. [83] a quantification of this effect with respect to the precursors concentration and the thermal annealing is made. The three possible situations for the band diagram in equilibrium short circuit condition are presented in the Figure 3.

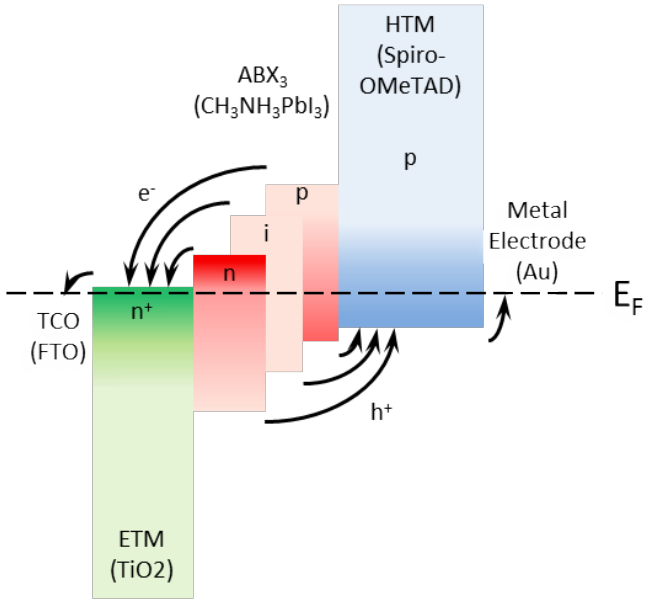

Figure 3. Representative PSCs energy band diagram in equilibrium short circuit condition. The different conductivity types found for $MAPbI_3$ are displayed with its respective charge separation paths. No band bending nor dipole layers were considered and only the band-gaps (color squares height) are scaled in an approximate alignment with the Fermi level (E_F).

Remarkably, an early work by Noh et al. [84] demonstrated the fabrication of colorful PSCs via band-gap tuning. Subsequently, new investigations on tunable structural color [85, 86] and neutral-colored devices [87, 88] have come out. These are important contributions towards building applications, such as in replacing windows, roofs, and even walls. Regarding the general performance, and as pointed in the early work by Yin et al. [89], the two other most characteristic perovskites are the hybrid halide $CH_3NH_3PbI_{3-x}Cl_x$ and the formamidinium (FA) cation composed $HC(NH_2)_2PbI_3$ [90]. About the former, the chlorine incorporation has been found to mainly improve the carrier transport across the heterojunction interfaces [91] while in $FAPbI_3$-based devices a broader absorption toward the infrared region [92] has been obtained. In this sense, the bandgap engineering is a clear pathway for augmenting PCE; for instance, band-gaps of have been reported [93, 94] by using tin compounds like $MASn_xPb_{1-x}I_3$ and $MASnI_3$, which is within the ideally optimal band-bap range (1.1 – 1.4 eV) for a single-junction device [95].

Furthermore, the development of lead-free PSCs is another crucial issue aiming at avoiding the risks due to the toxicity of Pb. Here three important alternatives can be highlighted as the most promising: (i) tin-based perovskites and (ii) antimony- and bismuth-based perovskites [96]. The use of $ASnX_3$ compounds has demonstrated improvement in stability and theoretical studies point out that an absorption coefficient similar to that of $MAPbI_3$ can be obtained. The Sb^- and Rb-based perovskites, on the other hand, has been proposed for high-bandgap PV application. A recent review by Shi et al. [97] deals with these subject.

Supplementing the above discussions and as a handy tool for practical use in the modeling and general comprehension of PSCs, the Table 1 present a summary of experimental parameters for the set of materials often used in this kind of devices.

Closing this section we recommend the work of Habibi et al. [134] for considering the fabrication and optimization of the absorber materials. Also the paper by Xinzhe et al. [135], that summarizes the recent progress in the synthesis of low-dimensional perovskites.

Table 1. Some experimental reports from literature on bandgap energy E_g, work function Φ, electron affinity χ_n and room temperature dielectric constant ϵ_r for several materials typically used in PSCs. Here Φ and χ_n are given in absolute values with respect to the vacuum level.

Materials	**Role**	E_g	Φ	χ_n	ϵ_r
		eV *ref.*	eV *ref.*	eV *ref.*	– *ref.*
FTO	TCO	4.0 – 4.5 [98,99]	4.4 – 5.0 [100,101]	5.6 [100]	3.7 [99]
ITO		3.5 – 4.0 [102,103]	4.4 – 4.8 [101,102,104]	4.1-4.5 [103]	4.0 [105]
TiO_2	ETM	3.2 [23]	3.7 – 4.2 [76,106]	3.6-4.1 [23,76]	18-22 [26]
PCBM		2.1 [107]	4.4 – 5.0 [108,109]	2.7-4.2 [110,111]*	3.4-3.9 [112,113]
Spiro-OMeTAD	HTM	3.0 – 3.6 [4,50]	3.9 – 5.2 [114,115]	2.11 [4]*	3.0 [116]
PEDOT		1.5 – 2.1 [61,117]	4.9-5.3 [115,118,119]	2.7-3.0 [117,120]*	3.5 [121]
$MAPbI_3$	Light	1.51 – 1.61 [65,67]	- -	3.9-4.8 [122,123]	22-35 [19,124,125]
$MAPbI_{1-x}Cl_x$	Absorber	1.57 – 1.74 [126,127]	- -	3.9 [123]	18-29 [125,128]
$FAPbI_3$		1.48 – 1.52 [19,65,127]	- -	4.2 [129,130]	47-49 [130,131]
A_g	Metal	- -	4.8 – 5.2 [81,132,133]	- -	- -
A_u	Contacts	- -	4.3-4.4 [81,132,133]	- -	- -

*Measurements made via cyclic voltammetry where a correction of LUMO relative to the vacuum level (−4.44 eV) is considered for the electrochemical scale.

III. DEGRADATION AND STABILITY OF PSCs

Early structural studies by Stoumpos et al. [65] stated that although $MAPbI_3$ is stable in air for months, meaning that its bulk properties are retained, an important surface effect take place given that it is affected by humidity and lose their crystalline luster after a couple of weeks. $MAPbI_3$ degradation in humid air proceeds by two competing reactions: (i) the generation of a $MAPbI_3$ hydrate phase by H_2O incorporation and (ii) the PbI_2 formation by the desorption of CH_3NH_3I species [136]. Subsequently, loss of CH_3NH_{3+} and I^- species and decomposition into $PbCO_3$, $Pb(OH)_2$, and PbO take place [137]. Illustratively, Noh et al. [84] reported an exposition to relative humidity of 55 % during 24 hours at room temperature as critical for the $MAPbI_3$ stability, which could be observed by an abrupt drop of more than the half of the performance efficiency in devices and a remarkable color change from dark brown to yellow. This feature can be observed in Figure 4.

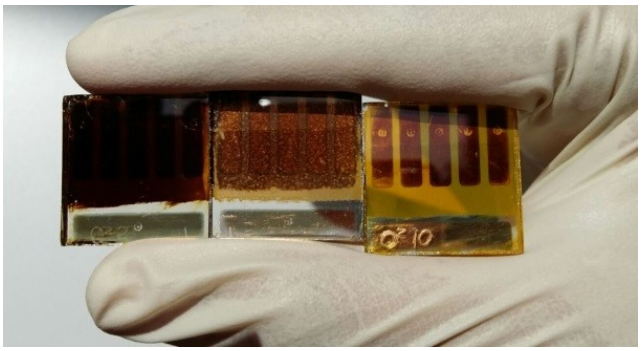

Figure 4. PSC before (dark brown on the left) and after (yellow on the right) long term degradation by exposure to normal environment conditions (air, dark, humidity of 25-40 %). The cell in the middle, with intermediate degree of degradation, shows the characteristic appearance of yellow dots.

Also the temperature plays an important role: while $MAPbI_3$ has a reported decomposition temperature of 300°C [66], the decomposition to PbI_2 at surfaces or grain boundaries has been found to occur at much lower temperatures as 150°C [138] and even 105°C [139]. More worrying, $MAPbI_3$ presents two crystalline phase transition around −111°C and 57°C, from orthorhombic to tetragonal and from tetragonal to cubic, respectively [65, 66, 140]. Regarding the first, the work by Jacobson et al. [141] discarded space applications due to the drastic PCE reduction toward the orthorhombic phase; while also recommended room temperature as the most profitable. On the other hand, considering that under sunny summer days the panels can reach over 80°C, the crystal instability of $MAPbX_3$ (X−Cl, Br, I) has gained the attention of several studies, as summarized by Niu et al. [142].

Anyway, there is still extensive research ongoing to understand the different and dominant PSCs degradation pathways, but clearly it was the moisture possibly the first major factor identified to affect $MAPbI_3$ stability in PSCs [143]. For preventing this, a primary strategy has been focused on the guarding and protecting of the absorber from external assaults by developing specialized functional barrier structures [144].

Nevertheless, provided the material is properly encapsulated (or measured in lab conditions under inert atmosphere) devices are still unstable. In particular, it has been shown that ionic transport induced by the electrical field can lead to the chemical reactivity of the external contacts with iodide ions [145, 146]. In addition, it is still not totally clear as whether $MAPbI_3$ is photostable [147].

Furthermore, the role of selective contacts on stability seems to be serious. For instance, an earlier study by T. Leijtens et al. [148] identified a critical instability in mesoporous $TiO_2/MAPbI_{3-x}Cl_x$ arising from light-induced desorption of surface-adsorbed oxygen, which was not present in meso-TiO_2 free devices. On the other hand, J.A. Christians et al. [149] found superior photocurrent stability when substituting spiro-OMeTAD by CuI. Also a tetrathiafulvalene derivative (TTF-1) as HTM was introduced by J. Liu et al. [150] as a stability improver. A more central change in the device architecture was proposed by S. Aharon et al. [151] who obtained best stability with $FAPbI_3$ as absorber material. The role of interface in stability is nicely reviewed in the article by Manspeaker et al. [152].

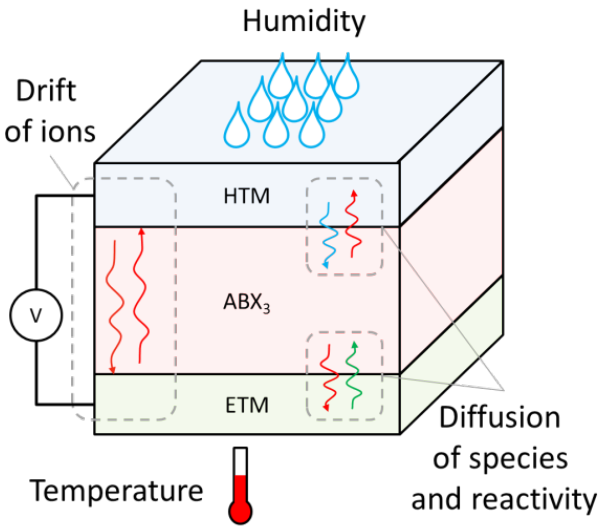

Figure 5. Main contributing factors in the degradation processes of PSCs.

Instructive reviews are also provided by Shahbazi & Wang [153], where the metals penetration is particularly mentioned, and Wang et al. [154], that underlines the standardization of testing protocols. More recently, the mini-review by Qin et al. [155] comments on the latest improvements that present up to 3000 hours stable PCE. Figure 5 summarizes the above noted main elements involved in degradation and instability of PSCs. These factors mutually complement each either and the path for the devices stabilization is to avoid their conjunction, or individual excess.

IV. HYSTERESIS OF PSCs

The current density-voltage ($J - V$) characterization constitutes a fundamental tool for understanding the

solar cells operation; and its performance under standard illumination conditions (air mass AM1.5, P_{in} = 100 mW·cm^{-2} [156]) is the established standard method for measuring the solar to electricity power conversion efficiency:

$$PCE = \frac{P_{max}}{P_{in}}, \tag{1}$$

being P_{max} the maxim attainable output power from the device (extracted from the $J-V$ curve). Among the most basic and widely used models for describing PV devices $J-V$ curves is that of equation [156,157]:

$$J = J_s\left(\exp\left[\frac{qV}{mk_BT} - 1\right] - 1\right) - J_{ph}, \tag{2}$$

where J_s is the saturation current density (A·cm^{-2}, where the area is that of the electrodes); q is the elementary charge; k_BT is the thermal voltage, m is the dimensionless diode ideality factor; and J_{ph} is the photocurrent (A·cm^{-2}, where the area is the light-absorbing). Each one of these parameters, in addition to others not included in equation 1 (e.g. series and shunt resistances), describes different mechanisms whose analysis constitutes a powerful tool for understanding the complete device.

Typically, for obtaining the experimental patterns that equation 2 describes -and hence calculate PCE via equation 1- a bias is applied across the device terminals sweeping the proper voltage range while current through an external circuit is been measured in the steady-state power output condition. However, it seems that such steady-state power output condition is not so easy to hold for $MAPbI_3$-based solar cells.

As described in the early work by Snaith and co-workers [158], the hysteresis phenomenon consists in the appearance of different $J-V$ curves depending on the scan direction and rate at which the bias is swept. For instance, as in Figure 6, we can label FR (forward to reverse) to the scan direction from open circuit to short-circuit and RF (reverse to forward) to the opposite bias sweep. In that convention it is apparent that the maxim output power when FR is larger than the corresponding in RF, as illustrated with the corresponding squares $P_{maxRF} < P_{maxFR}$ in Figure 6. Consequently, the reliability of the efficiency reports is not warrantied. Among the subsequent important contributions to the phenomenon description, Unger and co-workers [159] concluded that measurement delay time, and light and voltage bias conditions prior to measurement can all have a significant impact upon the shape of the measured $J-V$ curve, and by utilizing alternative selective contacts found that the contact interfaces have a big effect on transients in $MAPbI_3$-absorber devices. More successive descriptions and typical behaviors were reported, as nicely summarized by Ravishankar et al. [160]. Still without the proper understanding of the mechanisms behind this phenomenon, a first necessary step was to suggest special measurement protocols for avoiding unfeasible PCE reports. About this latter issue, the works by Kamat and co-workers [161] and Schmidt-Mende and co-workers [162] are of utmost significance.

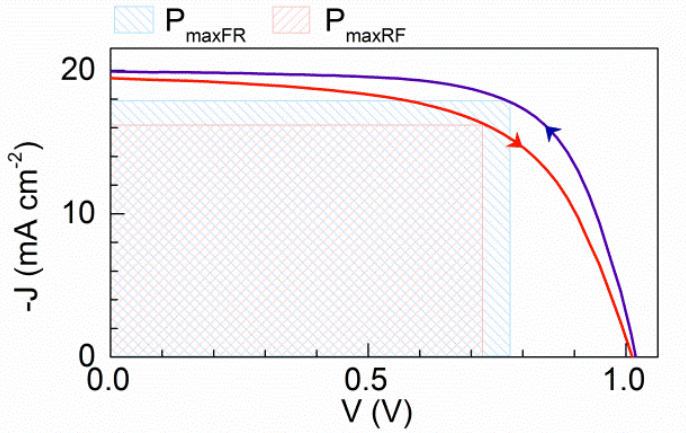

Figure 6. PSC $J-V$ curve in both bias scan directions (50 mV·s^{-1}) under 100 mW·cm^{-2} (AM1.5G) of illumination. The red (blue) gray square illustrates the corresponding maximum output power for the RF (FR) bias scan direction. The absolute current in the range between open circuit and short-circuit is often large when FR than when RF.

Regarding the clarifications for the hysteresis, Snaith and co-workers [158] first proposed three possible explanations: (i) filling and emptying of trap states, (ii) migration of excess ions, as interstitial defects (iodide or methylammonium), and/or (iii) ferroelectric effect. Accordingly, a lot of research contributed, and attempt to contribute yet, with evidence supporting one or another issue. However, at this point the most general criteria agreed in the cooperative confluence of dynamic and complex interactions between (i) electronic trapping and (ii) ionic mechanisms, leaving the (iii) ferroelectric effect as a possibly negligible factor.

Yet, favouring the ferroelectric behaviour, for example, Chen et al. [163] affirmed that the greater magnitude of hysteresis in the case of a planar heterojunction and Al_2O_3 scaffolds in comparison to mesoporous TiO_2 structures indicates the significance of the bulk property of perovskites rich in ferroelectric domains as an origin of hysteresis. A theoretical support to this hypothesis was afforded by Frost et al. [164,165] through *ab initio* molecular dynamics numerical simulations and also by Wei et al. [166] that interpreted the scan range and rate dependency as it is well explained by the ferroelectric diode model.

Other of those milestones worthy of mention in this race for the truth behind hysteresis, is Kim & Park's suggestion [167] that the origin of hysteresis is due to the characteristic capacitance C of $MAPbI_3$ by correlating the amount of hysteresis with the size of perovskite and mesoporous TiO_2 layers thickness. In other direction, Sanchez et al. [168] showed that the hysteresis is enhanced at high sweep rates (scan velocity dV/dt), and hence it could be a capacitive current effect:

$$J_{cap} = \frac{dQ}{dt} = C\frac{dV}{dt}, \tag{3}$$

which is a widely recognized feature in liquid electrolyte dye solar cells (DSCs). Importantly, as in equation 3, J_{cap} can be negative or positive depending on the charging or discharging given by the bias scan direction. In addition,

Almora et al. [169,170] studied the J_{cap} capacitive trend, but in dark conditions, linking the hysteretic behaviour with the capacitance excess observed at low frequencies, that correlated with ionic electrode polarization (see Figure 7). In addition, they checked the charging response of thick $MAPbI_3$ pellets revealing an interfacial double layer electrical structure formed by mobile ions at non-interacting Au contacts [171].

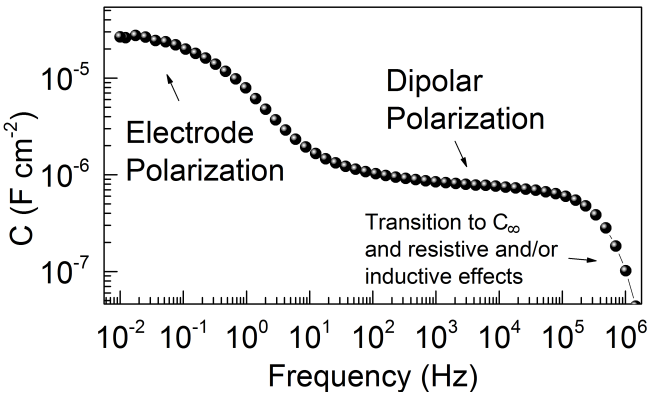

Figure 7. PSC capacitance spectrum measured via impedance spectroscopy in dark conditions, in short-circuit, at room air and temperature. Three main regions are indicated.

They also found that non-hysteretic samples (inverted structures) have not such capacitance increase at low frequency and furthermore identified non-capacitive hysteretic currents possibly related with reversible reactivity. In that formulation the curve was proposed to follow the law

$$J = J_{oper} + J_{cap} + J_{non-cap}, \tag{4}$$

where J_{oper} is the operation current, typically described by equation 2, and $J_{non-cap}$ can be assimilated to a step-like behavior

$$J_{non-cap} = J_{ncM}\left[1 + \exp\left(-\frac{q(V - V_0)}{mk_BT}\right)\right]^{-1}, \tag{5}$$

that attains J_{ncM} for positive potentials $V > V_0$. The characteristic voltage V_0 establishes the current onset and is related to a reaction potential.

Nevertheless, other more complex capacitive mechanisms actually occurs, and extra terms could be added to equation 3, such as VdC/dt. That's why linear trends in J_{cap} as a function of scan rate $s = dV/dt$ can be only obtained at short-circuit or low applied voltages. The thing is that time-changing capacitance was also pointed by Almora et al. [124] to behave similarly to the hysteresis in the curve, i.e. the capacitance evolve with the applied voltage. This, for instance, particularly hinders the performance of Mott-Schottky analysis. But despite this approach was clarifying, the nature of the processes that rule the capacitive features need further explanations.

Moreover, Tress and co-workers [172] argued, from their study on $J - V$ curve rate dependency and transient photocurrent, that the hysteretic behavior in timescales of seconds to minutes is most likely due to ions, which accumulate at the interfaces of the electrodes and screen the applied field independent of illumination. This was supported by conductance measurements by Beilsten-Edmands et al. [173] that specifically rejected the ferroelectric effect idea. Extra theoretical agreement was provided by van Reenen et al. [174] who achieve hysteresis in his modeled $J - V$ characteristics by including both ion migration and electronic charge traps, serving as recombination centers in a numerical drift-diffusion model. Also Richardson et al. [175] used simulations to join electrons, holes and defect mediated ion motion and obtain hysteretic $J - V$ patterns with the inclusion of the preconditioning procedures.

B. Chen et al. [176] reunited several evidences to explain that $J - V$ curve hysteresis should be due to two main processes: (i) capacitive effects associated with electrode polarization that provides a slow transient non-steady-state photocurrent and (ii) modification of interfacial barriers induced by ion migration that can modulate charge-collection efficiency so that it causes a pseudo-steady-state photocurrent, which changes according to previous voltage conditioning. As they point out, both phenomena are strongly influenced by ions accumulating at outer interfaces, but their electrical and photovoltaic effects are different: while the time scale for decay of capacitive current is on the order of seconds, the slow redistribution of mobile ions requires several minutes.

Finally, in the recent work by Bisquert and co-workers [160] a model was formulated based on the accumulation of surface electronic charge at forward bias that is released on voltage sweeping, causing extra current over the normal response. The charge shows a retarded dynamics due to the slow relaxation of the accompanying ionic charge, that produces variable shapes depending on scan rate or poling value and time. The equation of work for this surface polarization model is a particular case of equation 4 and can be written as

$$J = J_{oper} + C_{acc}\frac{dV_s}{dt} \tag{6}$$

where the accumulation capacitance C_{acc} is specified as a function of the surface polarization voltage V_s:

$$C_{acc} = \frac{q}{\gamma}\sqrt{\frac{2\epsilon_0\epsilon p_0}{k_BT}}\exp\left[\frac{qV_s}{\gamma k_BT}\right], \tag{7}$$

being p_0 the background hole density, $\epsilon_0\epsilon$ the dielectric permittivity and γ a parameter ideally close to 2. Moreover, V_s is a function of the constant built-in voltage and the applied voltage, $V_s = V - V_{bi}$, hence $dV/dt = dV_s/dt$.

V. CONCLUSIONS

The inclusion of hybrid lead halide perovskites like $MAPbI_3$ has been the key element for the fast emergence of perovskites solar cells. Next imminent steps are oriented to the optimizations of selective contact materials and structure

in general seeking the proper balance between performance, stability and production costs pursuing industrial scalability. About the origins of the current density-voltage curve hysteresis, further investigation needs to be done in order to clarify it. However, it seems that capacitive currents related with both electronic and ionic processes are the main responsible for such behavior.

ACKNOWLEDGEMENTS

We thank financial support by Ministerio de Economía y Competitividad (MINECO) of Spain under projects (MAT2016-76892-C3-1-R), and Generalitat Valenciana (Prometeo/2014/020). O. A. acknowledges Generalitat Valenciana for a grant (GRISOLIAP2014/035).

REFERENCES

[1] M. A. Green, Nat. Energy 1, 15015 (2016).
[2] M. A. Green, K. Emery, Y. Hishikawa, W. Warta, E. D. Dunlop, D. H. Levi, and A. W. Y. Ho-Baillie, Prog. Photovoltaics Res. Appl. 25, 3 (2017).
[3] R. M. Swanson, in Conference Record of the Thirty-first IEEE Photovoltaic Specialists Conference, 2005. (IEEE, Lake buena Vista, FL, USA, 2005), pp. 889.
[4] Y. Song, S. Lv, X. Liu, X. Li, S. Wang, H. Wei, D. Li, Y. Xiao, and Q. Meng, Chem. Commun. 50, 15239 (2014).
[5] M. Grätzel, J. Photochem. Photobiol., C 4, 145 (2003).
[6] J. Kim, G. Kim, T. K. Kim, S. Kwon, H. Back, J. Lee, S. H. Lee, H. Kang, and K. Lee, J. Mater. Chem. A 2, 17291 (2014).
[7] W. E. I. Sha, X. Ren, L. Chen, and W. C. H. Choy, Appl. Phys. Lett. 106, 221104 (2015).
[8] P. Gao, M. Gratzel, and M. K. Nazeeruddin, Energy Environ. Sci. 7, 2448 (2014).
[9] F. S. Galasso, R. Smoluchowski, and N. Kurti, Structure, Properties and Preparation of Perovskite-Type Compounds (Pergamon, London, 1969), International Series of Monographs in Solid State Physics.
[10] H. J. Snaith, J. Phys. Chem. Lett. 4, 3623 (2013).
[11] J.-H. Im, C.-R. Lee, J.-W. Lee, S.-W. Park, and N.-G. Park, Nanoscale 3, 4088 (2011).
[12] H.-S. Kim et al., Scientific Reports 2, 591 (2012).
[13] M. M. Lee, J. Teuscher, T. Miyasaka, T. N. Murakami, and H. J. Snaith, Science 338, 643 (2012).
[14] E. J. Juarez-Perez, R. S. Sanchez, L. Badia, G. Garcia-Belmonte, Y. S. Kang, I. Mora-Sero, and J. Bisquert, J. Phys. Chem. Lett. 5, 2390 (2014).
[15] R. Gottesman, E. Haltzi, L. Gouda, S. Tirosh, Y. Bouhadana, A. Zaban, E. Mosconi, and F. De Angelis, J. Phys. Chem. Lett. 5, 2662 (2014).
[16] P. Wang et al., Res. Chem. Intermed., 1 (2015).
[17] L. Wang, G.-R. Li, Q. Zhao, and X.-P. Gao, Energy Storage Materials 7, 40 (2017).
[18] L. Meng, J. You, T.-F. Guo, and Y. Yang, Acc. Chem. Res. 49, 155 (2016).
[19] N.-G. Park, M. Grätzel, and T. Miyasaka, Organic-Inorganic Halide Perovskite Photovoltaics: From Fundamentals to Device Architectures (Springer, Switzerland, 2016).
[20] Z. Zhou, S. Pang, Z. Liu, H. Xu, and G. Cui, J. Mater. Chem. A 3, 19205 (2015).
[21] L. Martinu and D. Poitras, J. Vac. Sci. Technol., A 18, 2619 (2000).
[22] N. G. Park, J. van de Lagemaat, and A. J. Frank, J. Phys. Chem. B 104, 8989 (2000).
[23] Z. Wang, U. Helmersson, and P.-O. Käll, Thin Solid Films 405, 50 (2002).
[24] A. Janotti, J. B. Varley, J. L. Lyons, and C. G. Van de Walle, in Functional Metal Oxide Nanostructures (Springer, New York, USA, 2012), pp. 23.
[25] B. S. Jeong, D. P. Norton, and J. D. Budai, Solid-State Electron. 47, 2275 (2003).
[26] A. Guerrero, E. J. Juarez-Perez, J. Bisquert, I. Mora-Sero, and G. Garcia-Belmonte, App. Phys. Lett. 105, 133902 (2014).
[27] J. Bisquert, Nanostructured Energy Devices: Equilibrium Concepts and Kinetics (CRC Press Taylor & Francis Group, Boca Raton, 2014).
[28] Y. Bai, I. Mora-Seró, F. De Angelis, J. Bisquert, and P. Wang, Chem. Rev. 114, 10095 (2014).
[29] D. V. Bavykin, J. M. Friedrich, and F. C. Walsh, Adv. Mater. 18, 2807 (2006).
[30] Y. Dai, C. M. Cobley, J. Zeng, Y. Sun, and Y. Xia, Nano Letters 9, 2455 (2009).
[31] M. He, D. Zheng, M. Wang, C. Lin, and Z. Lin, J. Mater. Chem. A 2, 5994 (2014).
[32] Y. Numata, Y. Sanehira, and T. Miyasaka, ACS Appl. Mater. Interfaces 8, 4608 (2016).
[33] A. Akbari, J. Hashemi, E. Mosconi, F. De Angelis, and M. Hakala, J. Mater. Chem. A 5, 2339 (2017).
[34] J.-M. Cha, J.-W. Lee, D.-Y. Son, H.-S. Kim, I.-H. Jang, and N.-G. Park, Nanoscale 8, 6341 (2016).
[35] G. Yang, C. Wang, H. Lei, X. Zheng, P. Qin, L. Xiong, X. Zhao, Y. Yan, and G. Fang, J. Mater. Chem. A 5, 1658 (2017).
[36] Z. Zhu, Y. Bai, X. Liu, C.-C. Chueh, S. Yang, and A. K. Y. Jen, Adv. Mater. 28, 6478 (2016).
[37] Q. Liu et al., Adv. Funct. Mater. 26, 6069 (2016).
[38] H. Zhou, Y. Shi, K. Wang, Q. Dong, X. Bai, Y. Xing, Y. Du, and T. Ma, J. Phys. Chem. C 119, 4600 (2015).
[39] M. A. Mahmud, N. K. Elumalai, M. B. Upama, D. Wang, K. H. Chan, M. Wright, C. Xu, F. Haque, and A. Uddin, Sol. Energy Mater. Sol. Cells 159, 251 (2017).
[40] J. Duan, Q. Xiong, H. Wang, J. Zhang, and J. Hu, J. Mater. Sci. Mater. Electron. 28, 60 (2017).
[41] J. You et al., Nat. Nanotechnol. 11, 75 (2016).
[42] D. Bi, S.-J. Moon, L. Haggman, G. Boschloo, L. Yang, E. M. J. Johansson, M. K. Nazeeruddin, M. Gratzel, and A. Hagfeldt, RSC Adv. 3, 18762 (2013).
[43] M. A. Mejía Escobar, S. Pathak, J. Liu, H. J. Snaith, and F. Jaramillo, ACS Appl. Mater. Interfaces 9, 2342 (2017).
[44] M. Acik and S. B. Darling, J. Mater. Chem. A 4, 6185 (2016).
[45] M. Hadadian et al., Adv. Mater. 28, 8681 (2016).

[46] S. Collavini and J. L. Delgado, Adv. Energy Mater., 1601000, 1601000 (2016).
[47] F. Zhang et al., Sol. Energy Mater. Sol. Cells 97, 71 (2012).
[48] G. Yang, H. Tao, P. Qin, W. Ke, and G. Fang, J. Mater. Chem. A 4, 3970 (2016).
[49] Y. Liu et al., Nano Lett. 15, 662 (2015).
[50] S. Fantacci, F. De Angelis, M. K. Nazeeruddin, and M. Grätzel, J. Phys. Chem. C 115, 23126 (2011).
[51] R. Schölin, M. H. Karlsson, S. K. Eriksson, H. Siegbahn, E. M. J. Johansson, and H. Rensmo, J. Phys. Chem. C 116, 26300 (2012).
[52] L. Calió, S. Kazim, M. Grätzel, and S. Ahmad, Angew. Chem. Int. Ed. 55, 14522 (2016).
[53] G. A. Sepalage, S. Meyer, A. R. Pascoe, A. D. Scully, U. Bach, Y.-B. Cheng, and L. Spiccia, Nano Energy 32, 310 (2017).
[54] I. S. Yang, M. R. Sohn, S. D. Sung, Y. J. Kim, Y. J. Yoo, J. Kim, and W. I. Lee, Nano Energy 32, 414 (2017).
[55] H. Rao, S. Ye, W. Sun, W. Yan, Y. Li, H. Peng, Z. Liu, Z. Bian, Y. Li, and C. Huang, Nano Energy 27, 51 (2016).
[56] Z. Zhu et al., Angew. Chem. Int. Ed. 53, 12571 (2014).
[57] P. Schulz, J. O. Tiepelt, J. A. Christians, I. Levine, E. Edri, E. M. Sanehira, G. Hodes, D. Cahen, and A. Kahn, ACS Appl. Mater. Interfaces 8, 31491 (2016).
[58] H. Sun, X. Hou, Q. Wei, H. Liu, K. Yang, W. Wang, Q. An, and Y. Rong, Chem. Commun. 52, 8099 (2016).
[59] R. Rajeswari, M. Mrinalini, S. Prasanthkumar, and L. Giribabu, Chem. Rec., n/a (2017).
[60] G. Greczynski, T. Kugler, M. Keil, W. Osikowicz, M. Fahlman, and W. R. Salaneck, J. Electron. Spectrosc. Relat. Phenom. 121, 1 (2001).
[61] Q. Pei, G. Zuccarello, M. Ahlskog, and O. Inganäs, Polymer 35, 1347 (1994).
[62] Y. Cao, G. Yu, C. Zhang, R. Menon, and A. J. Heeger, Synth. Met. 87, 171 (1997).
[63] M. Dietrich, J. Heinze, G. Heywang, and F. Jonas, J. Electroanal. Chem. 369, 87 (1994).
[64] W. Li, Z. Wang, F. Deschler, S. Gao, R. H. Friend, and A. K. Cheetham, Nat. Rev. Mater. 2, 16099, 16099 (2017).
[65] C. C. Stoumpos, C. D. Malliakas, and M. G. Kanatzidis, Inorg. Chem. 52, 9019 (2013).
[66] T. Baikie, Y. Fang, J. M. Kadro, M. Schreyer, F. Wei, S. G. Mhaisalkar, M. Graetzel, and T. J. White, J. Mater. Chem. A 1, 5628 (2013).
[67] Y. Yasuhiro, N. Toru, E. Masaru, W. Atsushi, and K. Yoshihiko, Appl. Phys. Express 7, 032302 (2014).
[68] T.-B. Song, Q. Chen, H. Zhou, C. Jiang, H.-H. Wang, Y. Yang, Y. Liu, and J. You, J. Mater. Chem. A 3, 9032 (2015).
[69] Y. Wang, Y. Zhang, P. Zhang, and W. Zhang, Phys. Chem. Chem. Phys. 17, 11516 (2015).
[70] S. Luo and W. A. Daoud, J. Mater. Chem. A 3, 8992 (2015).
[71] D. Song et al., J. Phys. Chem. C 119, 22812 (2015).
[72] W.-J. Yin, T. Shi, and Y. Yan, Appl. Phys. Lett. 104, 063903 (2014).
[73] S.-H. L. Jongseob Kim, Jung Hoon Lee, and Ki-Ha Hong, J. Phys. Chem. Lett. 5, 1312 (2014).
[74] W.-J. Yin, T. Shi, and Y. Yan, Adv. Mater. 26, 4653 (2014).
[75] J. Nelson, The Physics of Solar Cells (Imperial College Press, UK, 2003).
[76] P. Schulz, E. Edri, S. Kirmayer, G. Hodes, D. Cahen, and A. Kahn, Energy Environ. Sci. 7, 1377 (2014).
[77] J. Liu et al., J. Mater. Chem. A 3, 11750 (2015).
[78] R. Lindblad et al., J. Phys. Chem. C 119, 1818 (2015).
[79] J. H. Heo et al., Nat. Photon. 7, 486 (2013).
[80] S. Aharon, S. Gamliel, B. E. Cohen, and L. Etgar, Phys. Chem. Chem. Phys. (2014).
[81] X. Liu, C. Wang, L. Lyu, C. Wang, Z. Xiao, C. Bi, J. Huang, and Y. Gao, Phy. Chem. Chem. Phys. 17, 896 (2015).
[82] A. Dymshits, A. Henning, G. Segev, Y. Rosenwaks, and L. Etgar, Sci. Rep. 5, 8704 (2015).
[83] Q. Wang, Y. Shao, H. Xie, L. Lyu, X. Liu, Y. Gao, and J. Huang, Appl. Phys. Lett. 105, 163508 (2014).
[84] J. H. Noh, S. H. Im, J. H. Heo, T. N. Mandal, and S. I. Seok, Nano Lett. 13, 1764 (2013).
[85] W. Zhang, M. Anaya, G. Lozano, M. E. Calvo, M. B. Johnston, H. Míguez, and H. J. Snaith, Nano Lett. 15, 1698 (2015).
[86] E. S. Arinze, B. Qiu, N. Palmquist, Y. Cheng, Y. Lin, G. Nyirjesy, G. Qian, and S. M. Thon, Opt. Express 25, A101 (2017).
[87] G. E. Eperon, D. Bryant, J. Troughton, S. D. Stranks, M. B. Johnston, T. Watson, D. A. Worsley, and H. J. Snaith, J. Phys. Chem. Lett. 6, 129 (2015).
[88] L. Zhang, M. T. Hörantner, W. Zhang, Q. Yan, and H. J. Snaith, Sol. Energy Mater. Sol. Cells 160, 193 (2017).
[89] W.-J. Yin, J.-H. Yang, J. Kang, Y. Yan, and S.-H. Wei, Journal of Materials Chemistry A 3, 8926 (2015).
[90] W. S. Yang, J. H. Noh, N. J. Jeon, Y. C. Kim, S. Ryu, J. Seo, and S. I. Seok, Science 348, 1234 (2015).
[91] Q. Chen et al., Nat. Commun. 6 (2015).
[92] J.-W. Lee, D.-J. Seol, A.-N. Cho, and N.-G. Park, Adv. Mater. 26, 4991 (2014).
[93] Y. Ogomi et al., J. Phys. Chem. Lett. 5, 1004 (2014).
[94] N. K. Noel et al., Energy Environ. Sci. 7, 3061 (2014).
[95] F. Meillaud, A. Shah, C. Droz, E. Vallat-Sauvain, and C. Miazza, Sol. Energy Mater. Sol. Cells 90, 2952 (2006).
[96] P. V. Kamat, J. Bisquert, and J. Buriak, ACS Energy Lett. 2, 904 (2017).
[97] Z. Shi, J. Guo, Y. Chen, Q. Li, Y. Pan, H. Zhang, Y. Xia, and W. Huang, Adv. Mater., 1605005, 1605005 (2017).
[98] A. I. Martínez, L. Huerta, J. M. O. R. d. León, D. Acosta, O. Malik, and M. Aguilar, Journal of Physics D: Applied Physics 39, 5091 (2006).
[99] A. E. Rakhshani, Y. Makdisi, and H. A. Ramazaniyan, Journal of Applied Physics 83, 1049 (1998).
[100] M. G. Helander, M. T. Greiner, Z. B. Wang, W. M. Tang, and Z. H. Lu, J. Vac. Sci. Technol., A 29, 011019 (2011).
[101] A. Andersson, N. Johansson, P. Bröms, N. Yu, D. Lupo, and W. R. Salaneck, Adv. Mater. 10, 859 (1998).
[102] H. Y. Yu, X. D. Feng, D. Grozea, Z. H. Lu, R. N. S. Sodhi, A.-M. Hor, and H. Aziz, Applied Physics Letters 78, 2595 (2001).
[103] R. Singh, K. Rajkanan, D. E. Brodie, and J. H. Morgan, IEEE Transactions on Electron Devices 27, 656 (1980).

[104] J. S. Kim, B. Lägel, E. Moons, N. Johansson, I. D. Baikie, W. R. Salaneck, R. H. Friend, and F. Cacialli, Synthetic Metals 111–112, 311 (2000).
[105] I. Hamberg and C. G. Granqvist, J. Appl. Phys. 60, R123 (1986).
[106] A. Imanishi, E. Tsuji, and Y. Nakato, J. Phys. Chem. C 111, 2128 (2007).
[107] K. Akaike, K. Kanai, H. Yoshida, J. y. Tsutsumi, T. Nishi, N. Sato, Y. Ouchi, and K. Seki, J. Appl. Phys. 104, 023710 (2008).
[108] Y. Zhou, F. Zhang, K. Tvingstedt, S. Barrau, F. Li, W. Tian, and O. Inganäs, Appl. Phys. Lett. 92, 233308 (2008).
[109] M.-C. Wu, Y.-Y. Lin, S. Chen, H.-C. Liao, Y.-J. Wu, C.-W. Chen, Y.-F. Chen, and W.-F. Su, Chem. Phys. Lett. 468, 64 (2009).
[110] B. W. Larson, J. B. Whitaker, X.-B. Wang, A. A. Popov, G. Rumbles, N. Kopidakis, S. H. Strauss, and O. V. Boltalina, J. Phys. Chem. C 117, 14958 (2013).
[111] K. Kanai, K. Akaike, K. Koyasu, K. Sakai, T. Nishi, Y. Kamizuru, T. Nishi, Y. Ouchi, and K. Seki, Appl. Phys. A 95, 309 (2009).
[112] V. D. Mihailetchi, L. J. A. Koster, J. C. Hummelen, and P. W. M. Blom, Phys. Rev. Lett. 93, 216601 (2004).
[113] V. D. Mihailetchi, J. K. J. van Duren, P. W. M. Blom, J. C. Hummelen, R. A. J. Janssen, J. M. Kroon, M. T. Rispens, W. J. H. Verhees, and M. M. Wienk, Adv. Funct. Mater. 13, 43 (2003).
[114] P. Qin et al., Nanoscale 6, 1508 (2014).
[115] G. Y. Margulis, M. G. Christoforo, D. Lam, Z. M. Beiley, A. R. Bowring, C. D. Bailie, A. Salleo, and M. D. McGehee, Adv. Energy Mater. 3, 1657 (2013).
[116] D. Poplavskyy and J. Nelson, J. Appl. Phys. 93, 341 (2003).
[117] H. J. Spencer, P. J. Skabara, M. Giles, I. McCulloch, S. J. Coles, and M. B. Hursthouse, J. Mater. Chem. 15, 4783 (2005).
[118] R. A. Hatton, N. P. Blanchard, L. W. Tan, G. Latini, F. Cacialli, and S. R. P. Silva, Org. Electron. 10, 388 (2009).
[119] Y. Kim, A. M. Ballantyne, J. Nelson, and D. D. C. Bradley, Org. Electron. 10, 205 (2009).
[120] A. Marutaphan, Y. Seekaew, and C. Wongchoosuk, Nanoscale Research Letters 12, 90 (2017).
[121] F.-C. Chen, C.-W. Chu, J. He, Y. Yang, and J.-L. Lin, Appl. Phys. Lett. 85, 3295 (2004).
[122] J. Emara, T. Schnier, N. Pourdavoud, T. Riedl, K. Meerholz, and S. Olthof, Adv. Mater. 28, 553 (2016).
[123] C. Ludmila, U. Satoshi, J. A. Kumar, M. Tsutomu, N. Jotaro, K. Takaya, and S. Hiroshi, Chemistry Letters 44, 1089 (2015).
[124] O. Almora, C. Aranda, E. Mas-Marzá, and G. Garcia-Belmonte, Appl. Phys. Lett. 109, 173903 (2016).
[125] A. Poglitsch and D. Weber, J. Chem. Phys. 87, 6373 (1987).
[126] J. Chae, Q. Dong, J. Huang, and A. Centrone, Nano Letters 15, 8114 (2015).
[127] G. E. Eperon, S. D. Stranks, C. Menelaou, M. B. Johnston, L. M. Herz, and H. J. Snaith, Energy Environ. Sci. 7, 982 (2014).
[128] M. Samiee, S. Konduri, B. Ganapathy, R. Kottokkaran, H. A. Abbas, A. Kitahara, P. Joshi, L. Zhang, M. Noack, and V. Dalal, Applied Physics Letters 105, 153502 (2014).
[129] T. M. Koh, K. Fu, Y. Fang, S. Chen, T. C. Sum, N. Mathews, S. G. Mhaisalkar, P. P. Boix, and T. Baikie, J. Phys. Chem. C 118, 16458 (2014).
[130] A. A. Zhumekenov et al., ACS Energy Letters 1, 32 (2016).
[131] Q. Han et al., Adv. Mater. 28, 2253 (2016).
[132] H. B. Michaelson, J. Appl. Phys. 48, 4729 (1977).
[133] N. D. Orf, I. D. Baikie, O. Shapira, and Y. Fink, Appl. Phys. Lett. 94, 113504 (2009).
[134] M. Habibi, F. Zabihi, M. R. Ahmadian-Yazdi, and M. Eslamian, Renewable and Sustainable Energy Rev. 62, 1012 (2016).
[135] M. Xinzhe, P. Zhu, G. Shuai, and J. Zhu, J. Semicond. 38, 011004 (2017).
[136] M. Shirayama, M. Kato, T. Miyadera, T. Sugita, T. Fujiseki, S. Hara, H. Kadowaki, D. Murata, M. Chikamatsu, and H. Fujiwara, J. Appl. Phys. 119, 115501 (2016).
[137] W. Huang, J. S. Manser, P. V. Kamat, and S. Ptasinska, Chem. Mater. 28, 303 (2016).
[138] N. N. Toan, S. Saukko, and V. Lantto, Physica B 327, 279 (2003).
[139] Y. Shao, Z. Xiao, C. Bi, Y. Yuan, and J. Huang, Nat. Commun. 5 (2014).
[140] N. Onoda-Yamamuro, T. Matsuo, and H. Suga, J. Phys. Chem. Solids 53, 935 (1992).
[141] T. J. Jacobsson, W. Tress, J.-P. Correa-Baena, T. Edvinsson, and A. Hagfeldt, J. Phys. Chem. C 120, 11382 (2016).
[142] G. Niu, X. Guo, and L. Wang, J. Mater. Chem. A 3, 8970 (2015).
[143] S. Sun, T. Salim, N. Mathews, M. Duchamp, C. Boothroyd, G. Xing, T. C. Sum, and Y. M. Lam, Energy Environ. Sci. 7, 399 (2014).
[144] S. N. Habisreutinger, D. P. McMeekin, H. J. Snaith, and R. J. Nicholas, APL Materials 4, 091503 (2016).
[145] A. Guerrero, J. You, C. Aranda, Y. S. Kang, G. Garcia-Belmonte, H. Zhou, J. Bisquert, and Y. Yang, ACS Nano 10, 218 (2016).
[146] J. Carrillo, A. Guerrero, S. Rahimnejad, O. Almora, I. Zarazua, E. Mas-Marza, J. Bisquert, and G. Garcia-Belmonte, Adv. Energy Mater. 6, 1502246 (2016).
[147] D. Bryant, N. Aristidou, S. Pont, I. Sanchez-Molina, T. Chotchunangatchaval, S. Wheeler, J. R. Durrant, and S. A. Haque, Energy Environ. Sci. 9, 1655 (2016).
[148] T. Leijtens, G. E. Eperon, S. Pathak, A. Abate, M. M. Lee, and H. J. Snaith, Nat. Commun. 4 (2013).
[149] J. A. Christians, R. C. M. Fung, and P. V. Kamat, J. Am. Chem. Soc. 136, 758 (2014).
[150] S. Y. Li et al., Phys. Rev. B: Condens. Matter 64, 132505 (2001).
[151] S. Aharon, A. Dymshits, A. Rotem, and L. Etgar, J. Mater. Chem. A 3, 9171 (2015).
[152] C. Manspeaker, S. Venkatesan, A. Zakhidov, and K. S. Martirosyan, Curr. Opin. Chem. Eng. 15, 1 (2017).

[153] M. Shahbazi and H. Wang, Sol. Energy 123, 74 (2016).
[154] D. Wang, M. Wright, N. K. Elumalai, and A. Uddin, Solar Energy Materials and Solar Cells 147, 255 (2016).
[155] Q. Xiaojun, Z. Zhiguo, W. Yidan, W. Junbo, J. Qi, and Y. Jingbi, J. Semicond. 38, 011002 (2017).
[156] M. A. Green, Solar Cells. Operating principles, Technology and System Applications (Prentice-Hall, 1992).
[157] A. L. Fahrenbruch and R. H. Bube, Fundamentals of Solar Cells. Photovoltaic Solar Energy Conversion (Academic Press, UK, 1983).
[158] H. J. Snaith, A. Abate, J. M. Ball, G. E. Eperon, T. Leijtens, N. K. Noel, S. D. Stranks, J. T.-W. Wang, K. Wojciechowski, and W. Zhang, J. Phys. Chem. Lett. 5, 1511 (2014).
[159] E. L. Unger, E. T. Hoke, C. D. Bailie, W. H. Nguyen, A. R. Bowring, T. Heumuller, M. G. Christoforo, and M. D. McGehee, Energy Environ. Sci. 7, 3690 (2014).
[160] S. Ravishankar, O. Almora, C. Echeverría-Arrondo, E. Ghahremanirad, C. Aranda, A. Guerrero, F. Fabregat-Santiago, A. Zaban, G. Garcia-Belmonte, and J. Bisquert, J. Phys. Chem. Lett. 8, 915 (2017).
[161] J. A. Christians, J. S. Manser, and P. V. Kamat, J. Phys. Chem. Lett. 6, 852 (2015).
[162] E. Zimmermann et al., APL Mater. 4, 091901 (2016).
[163] H.-W. Chen, N. Sakai, M. Ikegami, and T. Miyasaka, J. Phys. Chem. Lett., 164 (2014).
[164] K. T. B. Jarvist M. Frost, Federico Brivio, Christopher H. Hendon, Mark van Schilfgaarde, and Aron Walsh, Nano Lett. 14, 2584 (2014).
[165] K. T. B. Jarvist M. Frost, and Aron Walsh, APL Mater. 2 (2014).
[166] J. Wei, Y. Zhao, H. Li, G. Li, J. Pan, D. Xu, Q. Zhao, and D. Yu, J. Phys. Chem. Lett. 5, 3937 (2014).
[167] H.-S. Kim and N.-G. Park, J. Phys. Chem. Lett. 5, 2927 (2014).
[168] R. S. Sanchez, V. Gonzalez-Pedro, J.-W. Lee, N.-G. Park, Y. S. Kang, I. Mora-Sero, and J. Bisquert, J. Phys. Chem. Lett. 5, 2357 (2014).
[169] O. Almora, I. Zarazua, E. Mas-Marza, I. Mora-Sero, J. Bisquert, and G. Garcia-Belmonte, J. Phys. Chem. Lett. 6, 1645 (2015).
[170] O. Almora, C. Aranda, I. Zarazua, A. Guerrero, and G. Garcia-Belmonte, ACS Energy Lett. 1, 209 (2016).
[171] O. Almora, A. Guerrero, and G. Garcia-Belmonte, Appl. Phys. Lett. 108, 043903 (2016).
[172] W. Tress, N. Marinova, T. Moehl, S. M. Zakeeruddin, M. K. Nazeeruddin, and M. Gratzel, Energy Environ. Sci. 8, 995 (2015).
[173] J. Beilsten-Edmands, G. E. Eperon, R. D. Johnson, H. J. Snaith, and P. G. Radaelli, Appl. Phys. Lett. 106, 173502 (2015).
[174] S. van Reenen, M. Kemerink, and H. J. Snaith, J. Phys. Chem. Lett. 6, 3808 (2015).
[175] G. Richardson, S. E. J. O'Kane, R. G. Niemann, T. A. Peltola, J. M. Foster, P. J. Cameron, and A. B. Walker, Energy Environ. Sci. 9, 1476 (2016).
[176] B. Chen, M. Yang, X. Zheng, C. Wu, W. Li, Y. Yan, J. Bisquert, G. Garcia-Belmonte, K. Zhu, and S. Priya, J. Phys. Chem. Lett. 6, 4693 (2015).